doi:10.1016/j.jmb.2005.02.019 J. Mol. Biol. (2005) 348, 113–125

JMB

Available online at www.sciencedirect.com

SCIENCE DIRECT®

ELSEVIER

Escherichia coli Purine Nucleoside Phosphorylase II, the Product of the *xapA* Gene

Gert Dandanell[1], Roman H. Szczepanowski[2,3], Borys Kierdaszuk[4] David Shugar[4,5] and Matthias Bochtler[2,3]*

[1]*Department of Biological Chemistry, Institute of Molecular Biology, Solvgade 83H, 1307 Copenhagen Denmark*

[2]*International Institute of Molecular and Cell Biology Trojdena 4, 02-109 Warsaw Poland*

[3]*Max-Planck-Institute for Molecular Cell Biology and Genetics, Pfotenhauerstr. 108 01309 Dresden, Germany*

[4]*Department of Biophysics Institute of Experimental Physics, University of Warsaw Żwirki i Wigury 93, 02-089 Warsaw, Poland*

[5]*Institute of Biochemistry and Biophysics, Polish Academy of Sciences, Pawinskiego 5a 02-106 Warsaw, Poland*

**Corresponding author*

Purine nucleoside phosphorylases (PNPs, E. C. 2.4.2.1) use orthophosphate to cleave the *N*-glycosidic bond of β-(deoxy)ribonucleosides to yield α-(deoxy)ribose 1-phosphate and the free purine base. *Escherichia coli* PNP-II, the product of the *xapA* gene, is similar to trimeric PNPs in sequence, but has been reported to migrate as a hexamer and to accept xanthosine with comparable efficiency to guanosine and inosine, the usual physiological substrates for trimeric PNPs. Here, we present a detailed biochemical characterization and the crystal structure of *E. coli* PNP-II. In three different crystal forms, PNP-II trimers dimerize, leading to a subunit arrangement that is qualitatively different from the "trimer of dimers" arrangement of conventional high molecular mass PNPs. Crystal structures are compatible with similar binding modes for guanine and xanthine, with a preference for the neutral over the monoanionic form of xanthine. A single amino acid exchange, tyrosine 191 to leucine, is sufficient to convert *E. coli* PNP-II into an enzyme with the specificity of conventional trimeric PNPs, but the reciprocal mutation in human PNP, valine 195 to tyrosine, does not elicit xanthosine phosphorylase activity in the human enzyme.

Keywords: PNP-II; *xapA* gene; biochemical characterization; crystal structure; phosphorolysis

Introduction

Purine nucleoside phosphorylases (PNP, EC 2.4.2.1) are ubiquitous enzymes, which catalyze the cleavage, by phosphorolysis, of the glycosidic bond of ribo and 2′-deoxyribo-purine nucleosides in the presence of inorganic phosphate (P_i), as follows:

$$\beta\text{-nucleoside} + P_i \rightleftharpoons \text{purine base} + \alpha\text{-D-ribose 1-phosphate}$$

Although the reaction is reversible *in vitro*, phosphorolysis is the predominant reaction *in vivo*, due to coupling with guanase and xanthosine oxidase, leading to formation of xanthine (Xan) and, finally, urate. PNP functions in the so-called purine salvage pathway, such that purine bases liberated by phosphorolysis are converted by purine phosphoribosyltransferases (PRTases) to their corresponding 5′-monophosphates.[1]

PNPs isolated from many different sources have, with some exceptions, been provisionally classified in two groups, based on molecular mass (*M*) and substrate specificity, as follows: (a) low molecular mass homotrimers ($M \sim 90$ kDa) active *versus* 6-oxopurines and their nucleosides, inosine (Ino) and guanosine (Guo), found in mammals and in some microorganisms; (b) high molecular mass homohexamers ($M \sim 110$–160 kDa), active *versus*

Abbreviations used: PNP, purine nucleoside phosphorylase; Gua, guanine; Guo, guanosine; Xan, xanthine; Xao, xanthosine; Hx, hypoxanthine; Ino, inosine; Ade, adenine; Ado, adenosine; P_i, orthophosphate; R1P, α-ribose-1-phosphate.

E-mail address of the corresponding author: mbochtler@iimcb.gov.pl

0022-2836/$ - see front matter

both 6-oxo and 6-amino-purines and their nucleosides, found in microorganisms.[1]

The most extensively studied of the latter group is the enzyme from *Escherichia coli*, the product of the *deoD* gene, referred to below as *E. coli* PNP-I, which cleaves adenosine (Ado) more effectively than Ino and Guo. It was then found that incubation of *E. coli* in the presence of xanthosine (Xao, but no other base or nucleoside) led to the appearance of a second enzyme, coded for by the induced *xapA* gene, and capable of efficiently cleaving the 6-oxopurine nucleosides Xao, Guo and Ino (see Figure 1), but not Ado.[2–4] This enzyme has been variously referred to as xanthosine phosphorylase and inosine-guanosine phosphorylase; we have chosen to refer to it as *E. coli* PNP-II, by analogy with some other microorganisms that contain more than one PNP.[1] Its sequence resembles that of mammalian PNPs, but has no similarity to that of the *E. coli* PNP-I,[5] for which Xao and Xan are not substrates (see Discussion, below).

PNP-I is a homohexamer in the crystal,[6,7] but its subunit composition in solution has not been unequivocally established.[1] By gel-filtration, PNP-II appears also to be a homohexamer, but with some evidence for co-existence of a trimeric form.[3,4]

Some of the properties of partially purified PNP-II have been described.[3,4,8] Unlike the enzyme from mammalian sources, for which Xao is a much weaker substrate than Guo,[9] *E. coli* PNP-II turns over Xao efficiently, with a reported K_m at neutral pH of 51 μM, as compared to 110 μM for Guo.[8]

An important factor hitherto overlooked, and to which attention has only recently been drawn,[1,9,10] particularly in an extensive review,[11] relates to the acid–base properties of Xan and Xao (see Figure 1). The neutral forms of Guo and Ino are predominantly 6-oxopurine nucleosides at neutral pH. Their monoanions ($pK_a \sim 9$), due to dissociation of the N(1)–H, are no longer 6-oxopurines. In striking contrast, Xan, with $pK_a = 7.5$, due to dissociation of the N(3)–H, is an equilibrium mixture of the neutral and monoanionic species at physiological pH; while Xao, with $pK_a = 5.7$, is predominantly a monoanion at physiological pH.[12,13] Furthermore, the monoanionic species of both are still 6-oxopurines (Figure 1). This has been fully taken into account in the present study of the properties of PNP-II, and its interaction with substrate ligands, largely by means of absorption and emission spectroscopy.

Results

Expression and purification

E. coli PNP-II is induced in xanthosine-containing media,[3] and is highly overexpressed in strain pCS59, which carries *xapA*, when induced with Xao.[14] To avoid contaminations of PNP-II preparations with Xao, a mutation in *xapA* was introduced that allows the expression of PNP-II in the absence of Xao. After harvesting and disrupting cells, PNP-II was enriched by ammonium sulfate precipitation and purified by ion-exchange

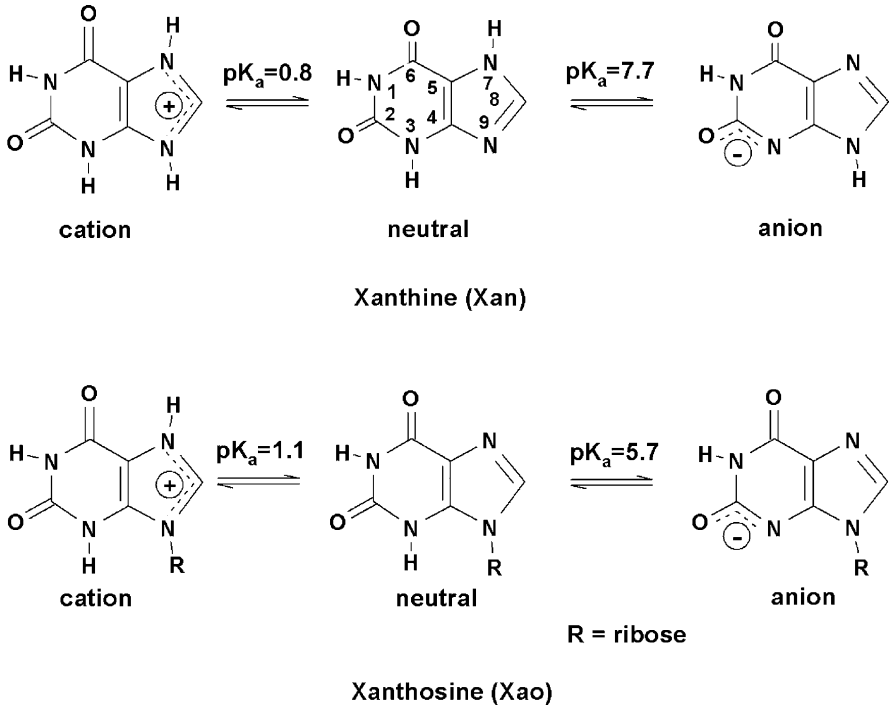

Figure 1. Structures of the neutral and monoanionic forms of xanthine (Xan) and xanthosine (Xao). The neutral and monoanionic forms of Xan exist in the prototropic tautomeric equilibrium of N(9)–H and N(7)–H,[34] and only the predominant tautomeric forms are shown. Note that the monoanions of Xan and Xao are still 6-oxopurines, like the neutral forms of Gua and Guo, and Hx and Ino.

Table 1. Data collection and refinement parameters

Ligands	Guanine, phosphate	Guanine, phosphate	Xanthine, sulfate
Space group	*P*3(2)21	*P*2(1)2(1)2	*P*2(1)2(1)2
a (Å)	71.3	73.4	93.4
b (Å)	71.3	98.5	150.4
c (Å)	267.5	116.6	155.2
No. protomers/asymmetric unit	3	3	6
Independent reflections (all/test)	14,985 (747)	26,636 (1352)	35,994 (1785)
Resolution (Å)	3.1	2.6	3.2
Completeness (%) (last shell)	99.9 (99.9)	99.9 (99.1)	97.8 (97.6)
R_{sym} (%) (last shell)	12.6 (38.2)	7.0 (32.8)	12.9 (35.7)
I/σ	11 (2.8)	20 (3.3)	9.9 (3.3)
B-factor from Wilson plot (Å^2)	64	49	49
R-factor (%)	24.6	24.1	25.0
R-free (%)	26.7	25.8	27.2
rmsd bond distance (Å)	0.02	0.01	0.01
rmsd bond angles (deg.)	1.8	1.8	1.3
rmsd *B* main-chain/side-chain (Å^2)	1.1/1.5	1.5/2.3	1.2/1.4
NCS rmsd coord. (Å)	< 0.02	< 0.02	< 0.02
Average *B* (Å^2)	42	37	28
Ramachandran core (%)	91.0	90.5	87.4
Ramachandran allowed (%)	8.0	8.7	11.8
Ramachandran add. allowed (%)	0.5	0.4	0.4
Ramachandran disallowed (%)	0.5	0.4	0.4

The densities for guanine and phosphate in the *P*3(2)21 crystal form are very weak.

chromatography as described in Materials and Methods.

Crystallization

E. coli PNP-II was crystallized in two crystal forms in the presence of Gua and phosphate, and in a third crystal form in the presence of Xan and sulfate (Table 1). All three crystal forms were grown at pH values between 8 and 9, which is not only above physiological, but also in the range where the activity of *E. coli* PNP-II drops strongly, particularly for Xan and Xao as substrates (see below). Crystals could not be grown at physiological pH, and no good crystals could be obtained in the presence of Xao, Guo or ribose 1-phosphate.

Structure determination

The crystal structure of *E. coli* PNP-II in the trigonal crystal form, which contains three protomers in the asymmetric unit, was solved by molecular replacement with trimeric calf spleen PNP as the search model.[15] After manual rebuilding, an improved model of *E. coli* PNP-II was used to solve the orthorhombic crystal form of PNP-II with Gua and phosphate, which also contained three protomers in the asymmetric unit. Intriguingly, PNP-II trimers in the asymmetric units of both crystal forms were packed in such a way that two trimers formed hexameric particles of 32 point symmetry in the crystal (Figure 2(a)). We therefore tried this hexameric arrangement as the search model for the orthorhombic crystal form with Xan and sulfate, which contains six protomers in the asymmetric unit. We found a strong molecular replacement solution, confirming the presence of this arrangement also for this crystal form. The models for all three crystal forms were manually improved and refined with NCS restraints to improve the observations to parameters ratio. The final models have acceptable *R*-factors (Table 1) and are essentially complete, except for a few residues at the N terminus and the loop from residue 60 to 68, that is disordered in most subunits and has not been built. As this loop is not in direct contact with the active site, the difference is not likely to be physiologically relevant. There is substantial disorder downstream of Asn239 in the trigonal crystal form, with poor or absent electron density for residues 240 to 262. As Asn239 is a ligand to the base, it is possible that poor order in this region and poor electron density for the base in this crystal form are interdependent. However, we note that crystal contacts prevent residues 240 to 262 from adopting the conformation seen in the other crystal forms, so that the disorder could simply be the result of crystal packing contacts.

Tertiary and quaternary structure

The presence of superimposable hexamers in all three crystal forms suggests that the hexamer is the predominant species under crystallization conditions, which are characterized by a high protein concentration, by a basic pH, and by the presence of substantial amounts of polyethylene glycol (see Materials and Methods), The arrangement of the *E. coli* PNP-II hexamer is very different from the arrangement of the *E. coli* PNP-I hexamer, even though both hexamers share the 32 point symmetry: PNP-II protomers are intimately interfaced within each ring, but make only limited contacts to the other ring (Figure 2(a)). In contrast, prior work on *E. coli* PNP-I[7] has shown that PNP-I protomers are held together by extensive inter-ring contacts, but

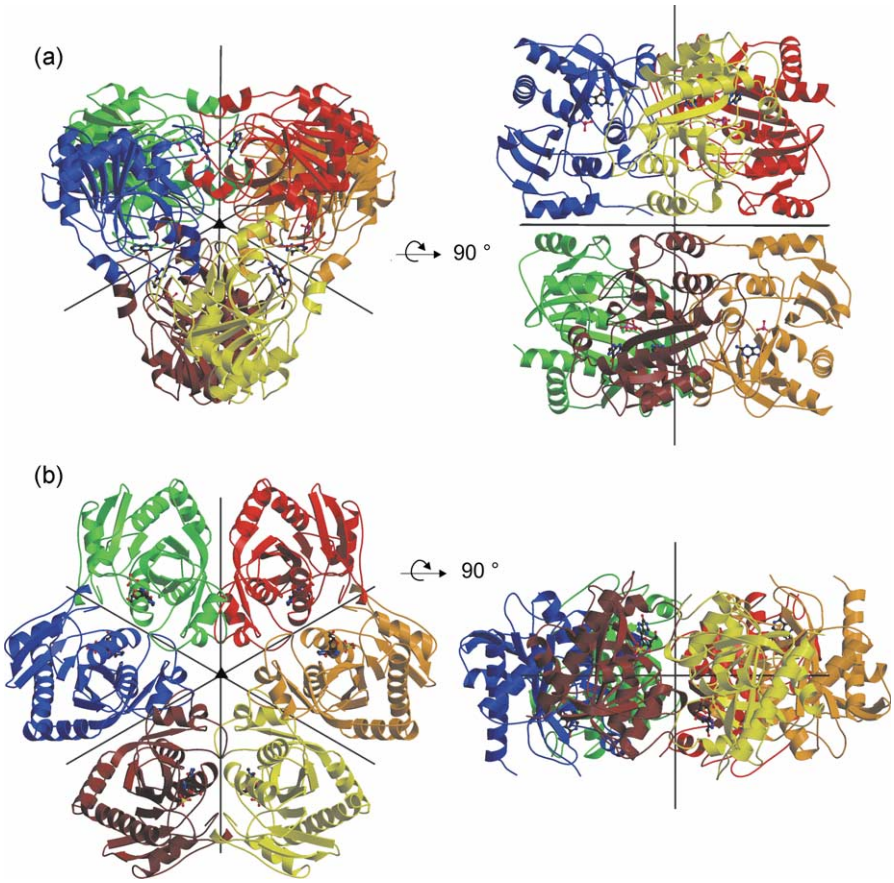

Figure 2. Top and side views of (a) *E. coli* PNP-II and (b) *E. coli* PNP-I in ribbon representation. Subunits are shown in different colors, and local symmetry axes are indicated. The ligands, guanine and phosphate in PNP-II, and formycin B and sulfate in PNP-I, are drawn in all-atom representation. (b) Based on the coordinates in 1A69.[7]

do not make any intra-ring contacts (Figure 2(b)). Thus, *E. coli* PNP-I can be described as a trimer of dimers, whereas *E. coli* PNP-II is best described as a dimer of trimers.

To assess the relevance of PNP-II trimer–trimer contacts in solution, we calculated the surface area that was buried by these contacts. We found a value of 2400 Å^2, roughly three times the surface area that was buried by a single protomer–protomer contact at the interface. The total contact area, 1200 Å^2, places the trimer–trimer contact in the twilight region of biologically meaningful protein–protein interactions[16] (Figure 2(a)).

Trimer–trimer interface regions between protomers are located in the immediate vicinity of local 2-fold axes, resulting in a duplication of contacts (Figure 3). Two protomer regions are involved, the N-terminal helix and a short stretch of residues around residue Pro55. A cluster of hydrophobic interactions is found in the immediate vicinity of the 2-fold axis: Phe12, Ile16 and Pro55 form a hydrophobic cluster that interacts with the equivalent hydrophobic cluster of residues in a subunit of the opposite ring. In particular, Pro55 stacks face to face with Phe12, a highly favored arrangement for proline–phenylalanine interactions.[17] Polar interactions are found slightly further away from the axis, where the Tyr20 OH donates a hydrogen bond to Asp15 O$^{\delta}$, and Thr19 O$^{\gamma}$ donates a hydrogen bond to Asp15 O. There is charge complementarity as well: the charged groups of Asp15 and Lys53 are 4–5 Å apart, and the distance between the charged groups of His8 and Glu52 is 6–7 Å. The former pair may form a salt-bridge, but the latter pair is so far apart that screening is likely to make this interaction marginal. We note that the residues at the trimer–trimer interface of *E. coli* PNP-II are not conserved in trimeric PNPs, despite strong overall sequence similarity. Thus, the structural data are compatible with the observation that *E. coli* PNP-II trimers show a tendency to dimerize, whereas the trimers of other sequence-related PNPs do not.

Phosphate-binding site

The trigonal and small orthorhombic crystal forms have a phosphate ion bound in exactly the location where it would be expected on the basis of trimeric PNP structures. In the large orthorhombic crystal form, grown in the absence of exogenously added phosphate, but in the presence of a large excess of sulfate, the density in the phosphate-binding site is presumably due to a bound sulfate ion. The environment of the phosphate or sulfate ion consists of residues Ser34, His87, Arg85 and

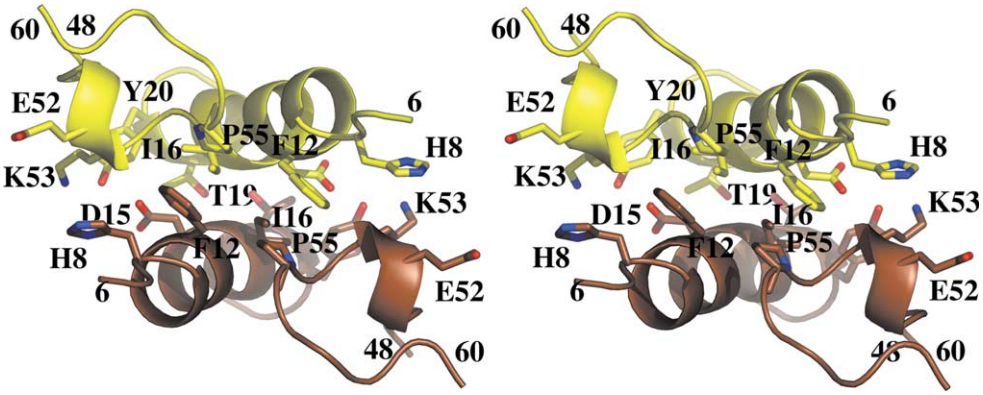

Figure 3. Detailed view of inter-ring protomer contacts along a local 2-fold axis, as seen from the inside of the particle. Color coding is consistent with Figure 2(a), and only selected residues are shown for clarity.

Ser216, all with their functional groups within hydrogen bonding distance of the phosphate molecule. As in trimeric PNP structures, one main-chain residue, Ala117 NH, donates a hydrogen bond to the phosphate. It has been argued for other PNPs that the histidine that coordinates the phosphate is part of a Glu-His-PO_4 catalytic triad.[18] This interpretation is possible for the *E. coli* PNP-II structure, where the $N^{\delta 1}$ of His87 is within hydrogen bonding distance of the side-chain carboxylate of Glu90 (Figure 4).

Purine-binding site

In all crystal structures, Gua and Xan interact with PNP-II *via* their hydrophobic faces and *via* hydrogen bonds in the plane of the bases. Phe196 packs against the purine base with a dihedral angle close to 90°, the most common arrangement for aromatic–aromatic interactions.[19] Met215 contacts the same face of the six-membered ring, and Thr254 comes close as well. The opposite face of the purine base contacts mostly backbone atoms of PNP-II, namely those of Ala118 and Gly214. In addition, the side-chain of Val213 contributes additional hydrophobic contacts to this face of the base (Figure 5(a)).

In the orthorhombic crystal form of PNP-II in complex with Gua, two residues that are conserved in trimeric PNPs, Asn239 and Glu197 in *E. coli* PNP-II numbering, are engaged in hydrogen bonding to the base. As Asn239 N^{δ} and Asn239 O^{δ} are indistinguishable crystallographically at 2.6 Å resolution, two rotamers can be modelled into the density for this residue. In the deposited model, Asn239 donates a hydrogen bond to Gua O6 (and to the main-chain carbonyl atom of Met240, not shown), and is ideally positioned to accept hydrogen bonds from Thr238 O^{γ} and from Gua N7, assuming that the N7–H form of Gua (which is in tautomeric equilibrium with the N9–H form of Gua in solution) is favored in the ligand-binding site of the enzyme (Figure 5(a) and (b)). As the X-ray data do not show hydrogen atoms and do not distinguish between nitrogen and oxygen atoms, an

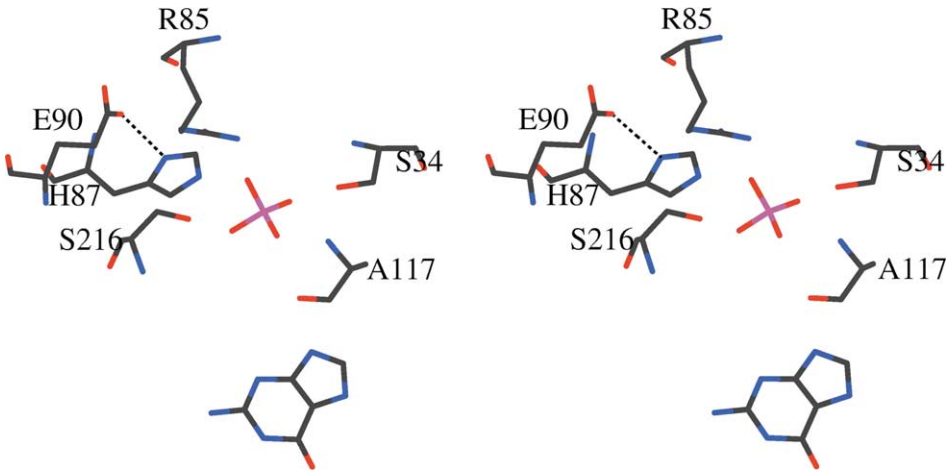

Figure 4. Stereo diagram of the phosphate binding site in *E. coli* PNP-II. Coloring is according to atom type, and the guanine ligand has been included for orientation. Note that the oxygen atoms of the phosphate in the center (red) are not resolved at the present resolution, and that only the position of the central P atom (pink) can be determined with certainty.

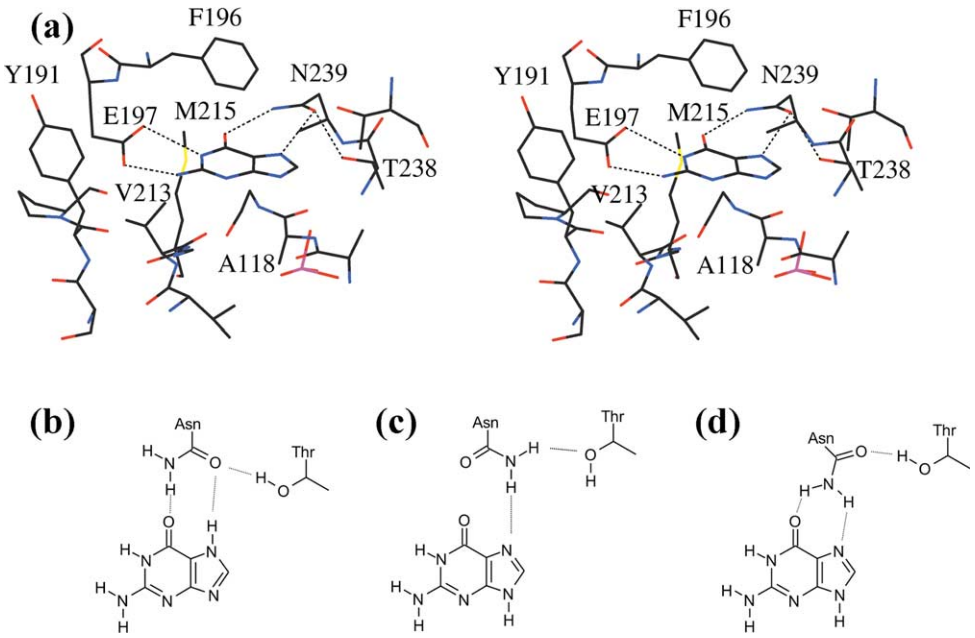

Figure 5. (a) Deposited model for *E. coli* PNP-II in complex with guanine for the small orthorhombic crystal form. (b) The interactions of guanine with Asn239 in the deposited model, and (c) an alternative interpretation that is also compatible with our data. The arrangement presented in (d) has been discussed for other trimeric PNPs, but is less compatible with the electron density for *E. coli* PNP-II.

alternative model, in which Asn239 N^{δ} donates hydrogen bonds to N7 and to Thr238 O^{γ}, as suggested for the ternary complex of bovine spleen PNP with Ino and sulfate[15] (Figure 5(c)), is equally possible. The data are less compatible with hydrogen bonds from Asn239 N^{δ} to both Gua O6 and N7 (Figure 5(d)), as originally suggested by modelling studies for complexes of human PNPs with purine bases[20] and, despite the limited resolution, argue against water-mediated, indirect contacts between Asn239 and the base (not shown). For the *E. coli* PNP-II in complex with Gua, at least in the orthorhombic crystal form, two additional hydrogen bonds can be assigned from Gua N1 and the exocyclic N2 to the terminal carboxylate of Glu197 (Figure 5(a)).

In the trigonal crystal form of *E. coli* PNP-II in complex with Gua, the residues downstream of Asn239 are poorly ordered or disordered, most probably as a result of crystal contacts that prevent this region from taking the conformation that is observed in the orthorhombic crystal form. The density for the base is poor, and it is doubtful whether the base-binding site is fully occupied at all. In the deposited model, a guanine molecule has been modelled in the position suggested by the much better defined density for the orthorhombic form, but support for this interpretation by the density is very limited.

In the orthorhombic crystal form with xanthine and sulfate, omit maps without model for the base indicate two uninterpreted regions of higher electron density, one where the cosubstrate α-D-ribose 1-phosphate would be expected to bind, and a second one that is consistent with the expected base binding site. The density for the former region may indicate the binding of a sulfate ion, present at 150 mM concentration in the buffer. The latter peak is likely to represent bound xanthine. The most parsimonious interpretation, a xanthine-binding mode that is similar to the guanine binding mode, is consistent with the observed electron density (Figure 6). Crystallographically, we cannot exclude alterations to the base binding mode, as between the original[21] and revised[22] binding modes for 8-azaxanthine to urate oxidase, but because most such rearrangements would alter the position of the N9, which is directly involved in catalysis, they are probably unlikely. If xanthine binds like guanine, it is most likely present in its neutral form. The monoanion would have its charge uncomfortably close to the terminal carboxylate of Glu197, but the neutral form of xanthine can donate a hydrogen bond from the N1 residue. The neutral species of Xan donates a hydrogen bond from N1 to this residue. A second hydrogen bond to Xan O2 from Glu197 would require protonation of the carboxylate, a very unlikely scenario, especially at the basic pH of the crystals. As diffraction data to 3.2 Å resolution are insufficient to assign details of a ligand-binding mode, we proceeded to characterize the binding mode of xanthine and xanthosine to *E. coli* PNP-II biochemically.

Xao, a substrate for wild-type PNP-II, but not PNP-II Y191L

It is not unusual for trimeric PNPs to accept Xao

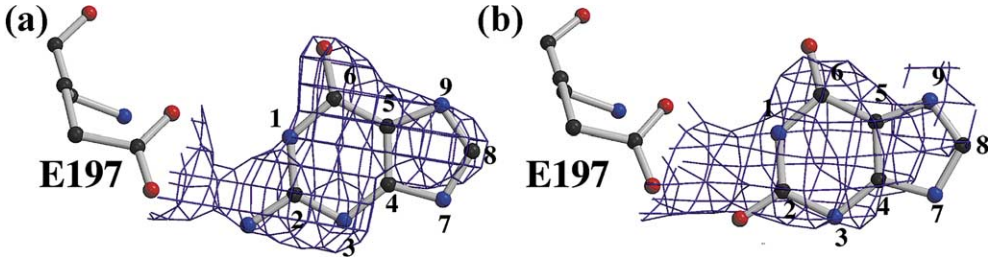

Figure 6. Omit densities for (a) the guanine and (b) the xanthine PNP-II ligands. For the density calculations, omit maps without the base in the models were calculated according to the CNS protocol that includes an annealing step to reduce phase bias. Maps were avaraged over all subunits in the orthorhombic crystals with (a) guanine and (b) xanthine, and have been contoured at 0.8σ. To make orientations comparable, whole subunits were superimposed, and Glu197 is indicated as a reference.

as a substrate, but at least for some of the best characterized PNPs, the affinity for Xan and Xao is 10–100-fold lower than for Gua and Guo.[9] In contrast, there is a broad consensus in the literature that Xao is an excellent substrate for *E. coli* PNP-II, even though there has been some debate about the ranking of substrates *in vitro* and the likely physiological substrate *in vivo*.[2,4,8] At pH 7.1, we find the tightest binding for Xao, and the highest maximal velocity for Guo as the substrate. V_{max}/K_m is similar for Guo and Xao, and substantially lower for Ino, due to weaker binding (Table 2).

A comparison of the active site of *E. coli* PNP-II with the active sites of previously crystallized trimeric PNPs does not readily explain the difference in substrate specificity. Active site superpositions and sequence alignments show that all residues in direct contact with the base are conserved between *E. coli* PNP-II and trimeric PNPs. However, we noted a tyrosine residue in *E. coli* PNP-II, in the vicinity of the active site (Figure 5(a)), that appeared to be unique to this enzyme. As this tyrosine, Y191, aligns with leucine, valine or methionine residues in other low molecular mass PNPs (alignment not shown), we introduced the PNP-II Y191L mutation into the expression plasmid, expressed the mutant in strain GD1525, which lacks *xapA*, the chromosomal gene for PNP-II, and characterized the purified protein. In striking contrast to the wild-type enzyme, the mutant had no detectable activity with Xao as substrate, but largely retained its activity against the other substrates, Ino and Guo, although with altered affinities and clearly reduced maximal velocity.

As this result suggested that residue 191 in *E. coli* PNP-II numbering (equivalent to residue 195 in human PNP numbering) is important for substrate selectivity, we next attempted to engineer a variant of human PNP with Xao phosphorylase activity by replacing the valine in this enzyme with tyrosine, the residue that is present in *E. coli* PNP-II. However, extracts with overexpressed mutant protein showed less activity against Xao than extracts with overexpressed wild-type protein, both in absolute numbers and in comparison with the rates for Ino phosphorolysis (data not shown). Consistent with the result for extracts, the purified V195Y mutant of human PNP was less active than wild-type human PNP (data not shown), demonstrating that human PNP had not been turned into a Xao phosphorylase.

Ado, a substrate for PNP-II N239D, but not wt-PNP-II

In prior studies with a mammalian PNP, Asn243, the equivalent of Asn239 in *E. coli* PNP-II, was shown to act as the selectivity filter for 6-oxo-purines.[23,24] To test the "selectivity" filter hypothesis for *E. coli* PNP-II, we cloned, expressed, purified and characterized the Asn239Asp variant of the enzyme. As predicted, the enzyme turned out to catalyze the phosphorolysis of Ado with moderate efficiency, and essentially lost all activity against the 6-oxo-purine substrates Ino, Xao and Guo (Table 2).

Substrate competition experiments

Substrate competition experiments were used to distinguish whether nucleosides that did not act as substrates had affinity for the enzyme, but failed to be turned over, or whether they failed altogether to bind to the enzyme. Ado, which is not a substrate for the wild-type PNP-II, appeared to be a weak inhibitor of the phosphorolysis of 150 μM Guo (IC_{50} ~ 850 μM). With the Y191L mutant, for which Ado and Xao are not substrates, the rate of phosphorolysis of 160 μM Guo at pH 7 was not detectably inhibited by 500 μM Ado or Xao, the latter of which is 95% in the anionic form at this pH. With the N239D mutant, phosphorolysis of 170 μM Ado was not detectably inhibited by 500 μM Guo, Xao, or Ino (which are not substrates). At this pH, Guo and Ino exist as the neutral forms (99%). In striking contrast, with the Y191L mutant, the initial rate of phosphorolysis of 230 μM Ino at pH 7 was inhibited about 50% in the presence of 100 μM Guo, further strongly accentuated as the reaction proceeded, pointing to involvement of the product of simultaneous phosphorolysis of Guo, i.e. Gua, as previously observed with the mammalian enzymes.[9]

Table 2. Kinetic parameters for phosphorolysis of Guo, Ino, Xao and Ado (in the presence of 10 mM P_i) for wild-type (WT) *E. coli* PNP-II, and its mutants Y191L and N239D, in 50 mM ammonium acetate buffer (pH 7.1) at 25 °C

	WT			Y191L			N239D		
Comp.	K_m (μM)	V_{max}	V_{max}/K_m	K_m (μM)	V_{max}	V_{max}/K_m	K_m (μM)	V_{max}	V_{max}/K_m
Ino	963(149)	11.9(9)	0.012(3)	231(62)	1.6(2)	0.0069(25)	–	[a]	–
Xao	72(11)	8.7(6)	0.120(25)	–	[a]	–	–	[a]	–
Guo	155(23)	14.2(9)	0.09(2)	249(64)	4.9(5)	0.020(7)	–	[a]	–
Ado	–	[a]	–	–	[a]	–	262(19)	0.215(6)	0.00082(8)

Values of Δε are 5300, 4130, 9600 and 2000 M^{-1} cm^{-1} for Guo-Gua (258 nm), Xao-Xan (242 nm), Ino-Hx-urate (300 nm) and Ado-Ade (260 nm), respectively. V_{max} values are in μmol/mg per minute; the standard deviations (in parentheses) refer to the last digit.

[a] No detectable substrate activity even with tenfold higher enzyme concentration.

The influence of pH on enzyme activity

A shift from slightly acidic to slightly basic pH converts Xan and Xao from their neutral to their monoanionic forms, but does not affect the charge states of Guo and Gua. A comparison of the pH-profiles for these four compounds should therefore indicate whether PNP-II binds the neutral or the monoanionic forms of Xan and Xao. Thus, pH profiles for the range from 5 to 10 for both the phosphorolysis reaction and the reverse synthetic reaction were recorded (Figure 7). For the pH range about 7, substrate concentrations were several-fold higher than measured K_m values, and thus reaction rates approximate V_{max} values. At the extremes of pH, the concentrations of Gua and Xan were limited by low solubility, and thus the decrease in reaction rate at these pH values may, in part, reflect reduced substrate concentration.

The V_{max} for phosphorolysis of Guo displays a broad pH optimum (6.5–7.5). At pH >7.5, corresponding to appearance of the monoanion (pK_a 9.2), there is a marked reduction in rate, and a steep drop at pH >9, where the monoanion of Guo predominates. Quite unexpected is the dramatic decrease in activity below pH 6.5, virtually zero at pH 6.0, a phenomenon not observed with PNP from other sources.[9] In this pH range, Guo exists uniquely in its neutral form (pK_a 2.2 for protonation).

With Xao as substrate, the pH profile is nearly symmetrical, with a broad optimum in the range 5.8–7.2. The marked decrease in V_{max} above pH 7 correlates with predominance of the Xao monoanion (pK_a 5.7). Note that below pH 6, where activity *versus* Guo is absent, V_{max} for Xao decreases markedly, notwithstanding that the neutral form predominates (pK_a ~0 for protonation).[10]

With Gua (pK_a 9.3) in the reverse synthetic

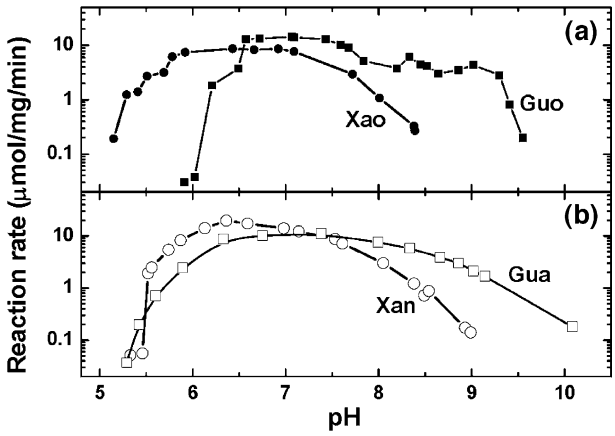

Figure 7. pH-dependence of activities of PNP-II from *E. coli* for (a) phosphorolysis of 0.8 mM Xao (●) and 0.8 mM Guo (■), and (b) the reverse synthetic reaction with 0.1 mM Xan (○) and 16 μM Gua (□). Measurements were made in 50 mM ammonium acetate buffer containing 10 mM P_i for phosphorolysis, and 1 mM R1P for the reverse reaction, at 25 °C. Reactions for Xao and Xan were monitored spectrophotometrically at 242 nm, and for Guo and Gua at 257 nm.

reaction, the pH optimum is again very broad, from pH 6.5 to 8. The reaction rate gradually decreases at pH >9, due to appearance of the monoanion (pK_a 9.3), but proceeds readily below pH 6 (pK_a 3.2 for protonation), where phosphorolysis of Guo is virtually absent (upper panel, Figure 7). The profile for Xan (pK_a 7.5) partially overlaps that for Gua, but activity drops precipitously below pH 5.8, at which phosphorolysis of Xao is fairly high.

Discussion

Oligomeric state

PNPs have been preliminarily classified as low molecular mass, trimeric, and high molecular mass, hexameric enzymes.[1] *E. coli* PNP-II departs from this classification, because it is similar to trimeric low molecular mass PNPs in sequence, protomer structure and specificity, yet is able to assemble into a high molecular mass hexamer by the dimerization of two trimers. Conservation of the dimerization interface in three, otherwise differently packed, crystal forms suggest that the dimerization interface could also play a role in solution. The description of the enzyme in the literature variously as a trimer and as a hexamer[3,4] supports this hypothesis. In our hands, at pH 5.5 and 7.6, only the high molecular mass, hexameric species of PNP-II was detectable by gel-filtration (data not shown).

Catalytic mechanism

The mechanistic details of the phosphorolysis reaction are somewhat controversial. In particular, the charge of the purine base in the transition state and the proton source for the reaction are still unclear (for a review, see Bzowska *et al.*[1]) The present study does not clarify the nature of the transition state, but shows that *E. coli* PNP-II, like trimeric PNPs, lacks a residue that would be chemically suitable and correctly positioned to act as a direct proton source, strongly suggesting that the proton is derived either from the co-substrate phosphate or from a solvent molecule.

Selectivity against adenine (Ade) and Ado

This study suggests that Asn239 in *E. coli* PNP-II acts as the selectivity filter for 6-oxo-purines and against 6-amino-purines, in perfect agreement with prior studies on sequence-related PNPs that suggested a similar role for the equivalent Asn243 in the human[24] and mouse[23] enzymes. Based on the substrate competition experiments, it appears that Ado can act as a weak inhibitor of Guo phosphorolysis, and therefore seems to have limited affinity for the enzyme, implying that the lack of Ado phosphorolysis activity is, in part, due to impaired turnover.

Although expected in the context of trimeric PNPs, the asparagine-mediated selectivity for Gua and Xan, and against Ade, is remarkable in the light of a survey of the entire Protein Data Bank (PDB) for interactions of purine bases with amino acid side-chains. According to this survey, and in contrast to the situation for trimeric PNPs, asparagine and glutamine form significant interaction clusters with adenine, but not with Gua.[25] We note that the choice of rotamer for Asn239 in Figure 5(b) naturally predicts the selectivity for 6-oxo and against 6-amino-purines, whereas the alternative arrangement in Figure 5(c) is harder to reconcile with the observed substrate specificity. Moreover, the arrangement in Figure 5(b), but not in Figure 5(c), favors protonation of the N7 of the purine base, a necessary step in the catalytic cycle.

Preference for Xan and Xao in their neutral forms

The crystal structures of *E. coli* PNP-II with Gua and Xan suggest that the binding modes for the two compounds are similar. If the Xan monoanion was the substrate, this binding mode would juxtapose the negative charge of the Xan monoanion with the negative charge of the terminal carboxylate of Glu197. Hence, it is very likely that either Xan is present in the neutral form, or alternatively, that Glu197 is protonated. If Glu197 is taken to be deprotonated, its negative charge would be expected to disfavor dissociation of the N3 acidic proton of Xan or Xao, effectively causing an upshift for their pK_a values in the presence of enzyme.

As the crystallographic data for the *E. coli* PNP-II complex were obtained at 3.2 Å resolution for a crystal that was grown at pH 9.0, where the enzyme is almost inactive with Xan as the substrate, it is reassuring that binding of the neutral forms of Xao and Xan is consistent with the pH profiles for the phosphorolytic and reverse synthetic reactions. The pH optima for the reactions with Xao and Xan are more acidic than the reaction rates for Guo and Gua. At basic pH values, where Xao (pK_a 5.7) and Xan (pK_a 7.5) would be expected to be present as monoanions in solution,[9] the reaction rates for these two compounds are much lower than the corresponding reaction rates for Guo and Gua (Figure 7). Although pK values may be perturbed in the presence of enzyme, and although the differences in phosphorolysis rates of Xao and Guo at acidic pH remain unexplained, all data for *E. coli* PNP-II are consistent with the conclusion that the neutral forms of Xao and Xan are the predominant, and probably exclusive, substrates of the enzyme. Similar conclusions have been drawn for calf and human PNPs that use Xao and Xan with much lower efficiency, but still accept them as substrates and for *Salmonella typhimurium* nucleoside hydrolase RihC.[9,36]

The broadened substrate specificity of *E. coli* PNP-II

The crystal structure of *E. coli* PNP-II shows that the broadened substrate specificity of the enzyme

does not result from a variation in any of the residues that are in direct contact with the substrate. Based on sequence comparisons, we initially hypothesized that Tyr191, a residue that is unique for the *E. coli* enzyme and located in the second shell of residues around the base, could displace Glu197 in the complex with Xan and donate a hydrogen bond to the monoanionic form. Both the biochemcial and the crystallographic data exclude this original "tyrosine flip" hypothesis. From the pH profiles, it appears that the monoanionic forms of Xan and Xao do not act as substrates, and the crystallographic data for the *E. coli* PNP-II in complex with Xan show robust density for the tyrosine side-chain pointing away from the base. A limited, mechanistically undefined, role for Tyr191 in the broader substrate specificity of *E. coli* PNP-II is nevertheless suggested by the lack of Xao phosphorylase activity in the mutant. However, the failure of the reciprocal experiment to convert human PNP-II into a Xao phosphorylase by the introduction of tyrosine in the equivalent position of the human enzyme shows that other, still unidentified, residues also play a role in determining substrate specificity.

Comparison with phosphoribosyltransferases

The unusually expanded specificity of *E. coli* PNP-II has an interesting parallel in purine phosphoribosyltransferases. Most enzymes in this class accept hypoxanthine and Gua as substrates, but cannot process Xan.[26,27] In contrast, the enzyme from *Toxaplasma gondii* readily accepts Xan, and is therefore referred to as hypoxanthine-guanine-xanthine phosphoribosyltransferase (HGXPRTase).[28] The expanded substrate specificity of the parasite enzyme has been studied, albeit without regard to the charge state of the base. The crystal structure of HGXPRTase in complex with Xao monophosphate[29] shows that the crucial exocyclic O2 of Xan contacts an amide nitrogen of the main chain. Consequently, no obvious residue change could be identified that would account for the expanded substrate specificity of HGXPRTase. Very recently, random mutagenesis was used to generate a variant of the human phosphoribosyltransferase that has expanded substrate specificity similar to that of the parasite enzyme.[30] Interestingly, the ability to phosphoribosylate xanthine depends on the mutation of a residue that is not in direct contact with the base,[30] again suggesting that long-range, indirect effects play an important role.

Phosphoribosyltransferases and purine nucleoside phosphorylases are unrelated in fold and catalytic mechanism, so that mutations in one group of enzymes have no direct equivalent in the other group of enzymes. Nevertheless, the indirect modulation of substrate specificity by residues that are not in direct contact with the base appears to be a shared feature of both enzyme families that clearly requires further study.

Materials and Methods

Bacterial strains and plasmid vectors

To avoid problems with PNP-I (encoded by *deoD*), GD1424 (BL21/DE3, *deoD zjj*::Tn*10*) was constructed by transduction by P1 phages grown on SØ6416.[14] To avoid expression of both wild-type PNP (chromosomal) and mutant PNP, GD1525 (BL21/DE3, *deoD zjj*::Tn*10*, Δ*xapABR*::*kan*^{R}) was constructed by transducing GD1424 with P1 phages grown on GD749.[14] Plasmids were transformed into GD1424 (PNP-II) or GD1524 (mutant-PNPs) and grown in LB medium supplemented with 150 μg/ml of ampicillin at 37 °C.

pCS59 carries *xapABR* and highly overexpresses PNP-II when induced with xanthine.[14] In order to avoid Xao in the enzyme preparation, a XapR9 mutation was introduced which induced PNP-II expression in the absence of Xao. pCS59 was digested with SacI and SalI, and ligated to two PCR fragments, resulting in pGD265. One PCR fragment was produced by amplifying pCS59 using primers A (5′-CTGCATGAGATACAACAGGTATCGC) and B (5′ GGGCCCATGGTCGTTTCCTTGTCGCATCAT TTGG) which, after digestion with SacI and NcoI, carries the 3′ end of *xapA* with an NcoI site. The second PCR fragment was produced by amplifying pCJ2F[31] using primers C (5′-ACTTAACCATGGAACGCGTATACAGA AC) and D (5′-TTGCGTCGACGCCTGATGCGCTTCA CTTAGC) which, after digestion with NcoI and SalI, carries *xapR9* with a 5′-NcoI site.

All mutations were introduced into PGD265 using the quickchange method of Stratagene, USA. pGD265(E197K), pGD265(E197Q), pGD265(Y191L) and pGD265(N239D) were constructed with the following and their complementary primers: (5′-CATGCGAAT TTCCGCCGCAGTCTTGAAATTCGGCCCCG), (5′-CGG GGCCGAATTTCCAGACTGCGGCGGAAATTCGCATG), (5′-GGAGGGCGTGTTCGTCTCGCTGCCGGGGCCGAA TTTC) and (5′-GCGGTCTCTGCGATTACCGATATGG CGGAAGGTTTAAGC), respectively. All constructions were verified by DNA sequencing, using the BigDyeTM terminator cycle sequencing kit and an ABI PRISMTM 310 Genetic Analyzer (PE Applied Biosystems, Warrington, Great Britain).

Expression and purification of PNP-II and mutant PNP-II

Cells from 500 ml overnight cultures (LB supplemented with 150 μg/ml of ampicillin) were harvested by centrifugation for 20 minutes at 9000 rpm (Sorval GS-3 rotor), washed with 0.9% (w/v) NaCl, and resuspended in buffer A (100 mM Tris–HCl (pH 8.5), 2 mM EDTA, 5 mM mercaptoethanol). Cells were disrupted by sonication and cell debris was removed by centrifugation for ten minutes at 10,000 rpm (Sorval SS34 rotor). Streptomycin sulfate was added to a final concentration of 1% (w/v), and the extract incubated on ice for 30 minutes. The extract was centrifuged for 15 minutes at 15,000 rpm (Sorval SS34 rotor) and the pH of the supernatant was adjusted to pH 6.4 with 10% (v/v) acetic acid. After ten minutes on ice, debris was removed by centrifugation for 15 minutes at 15,000 rpm (Sorval SS34 rotor). PNP-II was precipitated by adding ammonium sulfate to a final concentration of 33%. Some of the mutants were not as highly overexpressed as PNP-II, and the ammonium sulfate concentration had to be increased up to 45% to precipitate them. After incubation on ice for 60 minutes, PNP-II was collected by centrifugation for 30 minutes at

15,000 rpm (Sorval SS34 rotor). PNP-II was resuspended in buffer B (25 mM K-PO_4, 5 mM mercaptoethanol, pH 7.4) while mutant-PNP-II was resuspended in buffer BG (buffer B+5% glycerol). PNP(Y191L) was found to be very unstable in buffer B but could be stabilized by glycerol. The solubilized protein was dialyzed overnight in buffer A and applied on a 25 ml MonoQ-FF column (Amersham Pharmacia Biotech) attached to an FPLC apparatus (BioRad, USA). The column was washed with 100 ml of buffer B, and eluted with a linear gradient to buffer B +1 M NaCl (buffer BG was used for mutant PNPs). PNP-II eluted at approximately 300 mM NaCl. Fractions containing PNP-II were identified by SDS-PAGE and pooled. DTT and glycerol were added to final concentrations of 1 mM and 25%, respectively. By SDS-PAGE, PNP-II was estimated to be >98% pure, while the mutant PNPs were >95% pure. Variations in purity appeared to correlate with variations in the level of overexpression. Protein concentration was calculated from the absorbance at 280 nm. Purification from 500 ml of culture typically gave 80–150 mg of enzyme.

Enzyme kinetics

Guo, Ino, mono- and disodium phosphate and α-D-ribose 1-phosphate (R1P) were from Sigma (St. Louis, MO, USA), and Xao and Xan were from Serva (Heidelberg, Germany). Purity of compounds was confirmed by chromatography and pH-dependent UV absorption spectra. Xao showed isosbestic points at 239 nm, 258 nm and 270 nm, and Xan at 252.5 and 274 nm. All solutions were prepared with high-quality Milli-Q water, using reagents of the highest quality. Solutions contained background contaminant phosphate, ≤1 μM, estimated spectrophotometrically,[35] hence sufficiently low as not to affect overall results, and referred to as P_i-free controls.

Ammonium acetate buffers (Sigma, USA) were selected to avoid buffer effects on enzyme activity, previously noted with Tris and other buffers (see Stoychev *et al.*[9] and references cited therein).

Measurements of pH (±0.05) were carried out with a CP315 m (Elmetron, Poland) pH-meter equipped with a combination semi-micro electrode (Orion, UK) and temperature sensor. Ultraviolet absorption was monitored with a Varian (Australia) Cary Bio-50 recording instrument, fitted with a thermostatically controlled cell compartment, using 1, 2, 5 or 10 mm pathlength cuvettes. Concentrations of substrates and protein (hexameric holoenzyme) were determined spectrophotometrically at pH 7.0 for: PNP-II λ_{max} 280 nm (ε 24.2×10^3); Guo λ_{max} 253 nm (ε 13.7×10^3); Ino λ_{max} 248 nm (ε 12.3×10^3); Ado λ_{max} 259 nm (ε 15.4×10^3); Gua λ_{max} 246 nm (ε 10.7×10^3); Hx λ_{max} 250 nm (ε 10.7×10^3); Ade λ_{max} 261 nm (ε 13.4×10^3). For Xao (pH 9) λ_{max} 248 and 278 nm (ε 10.1×10^3 and 9.0×10^3), and for Xan (pH 10) λ_{max} 241 and 278 nm (ε 9.0×10^3 and 9.3×10^3).

Phosphorolysis was monitored spectrophotometrically at 25 °C in 50 mM ammonium acetate buffer in the presence of 10 mM P_i (substrate saturation well above K_m <1 mM) by following the changes in absorption of Xao to Xan at 242 nm, using values of Δε determined at each pH; for Guo to Gua at 257 nm, with Δε 4600 in the pH range 3.6–8.5; and for Ado to Ade at 260 nm, with Δε 2000 at pH 7. Phosphorolysis of Ino was followed spectrophotometrically by coupling with Xan oxidase. The absorption spectra of phosphorolysis of Xao and Guo showed isosbestic points at all tested pH values. For example, at pH 5.7, isosbestic points were at 223, 260 and 279 nm for Xao, and at 240 and 287.5 nm for Guo.

The reverse synthetic reaction was monitored in the presence of 1 mM R1P (substrate saturation). For pH effects on enzyme activity, activities were monitored with 0.8 mM Xao or Guo, and 10 mM P_i, for phosphorolysis; and Xan (0.8 mM) or Gua (100 μM) and R1P (1 mM) for the reverse reaction. Concentrations of substrates were saturated in the pH range 5–8 (for Xao) and 5.0–7.5 (for Xan), where they are at least threefold higher than the K_m values.

Kinetic constants were determined using the initial rate method. Initial rates (v) were determined from linear regression fitting to at least ten experimental points with an accuracy of 5% or less. The values of K_m and V_{max} were determined from non-linear regression fitting of the Michaelis–Menten equation in the form of Eaddie–Hofstee plots:

$$v = V_{max} - K_m(v/[S])$$

Crystallization and structure determination

Crystals were grown by vapor diffusion at room temperature in sitting drops. In all experiments, 2 μl of reservoir buffer was mixed with a 15 mg/ml protein solution in 50 mM Tris (pH 7.5), 100 mM KCl in the presence of the appropriate purine base. Crystals typically appeared after several weeks.

The first crystals were obtained from 50 mM Tris (pH 8.2), 14% PEG 4000, and were grown from a protein solution saturated with Gua and supplemented with 1 mM phosphate. Crystals were small and diffracted poorly in-house, but could be flash-cryocooled after equilibrating with cryobuffer consisting of 17 μl of reservoir solution and 3 μl of (2*R*,3*R*)-(−)-2,3-butanediol. The original diffraction pattern was highly smeared, but improved dramatically after a brief annealing step in cryobuffer. Following this protocol, a dataset for the Gua complex to 3.1 Å resolution could be collected on EMBL X11, DESY. The unit cell was trigonal with cell constants 71.3 Å×71.3 Å×267.5 Å, and contained one trimer per asymmetric unit. With the trimer of bovine spleen PNP (PDB-accession code 4PNP)[15] as the search model for molecular replacement, three clear rotational solutions (corresponding to the three ways two trimers can be superimposed) were found. Subsequent translational searches showed a clear signal/noise ratio only for space group $P3_221$, consistent with observed extinctions on the 00l-line. The resulting model was corrected through iterative rebuilding in O[32] and refinement with CNS.[33] The final model lacks residues 61–67 and 240–262 that are poorly defined in this crystal form. The phosphate and guanine ligands have been included in the final model for all three protomers in the asymmetric unit, even though the density for them is poor, and their binding sites may only be partially occupied.

Orthorhombic crystals with cell constants 73.4 Å, 98.5 Å and 116.6 Å were obtained from 50 mM glycine (pH 9.0), 24% PEG 4000 in the presence of stoichiometric amounts of Gua (1:1 ratio of Gua to monomer) and 1 mM phosphate. The resolution limit was poor if crystals were mounted at 16 °C in capillaries, but improved to 2.6 Å after a quick pass of the crystal through cryobuffer (50 mM glycine (pH 9.0), 45% PEG 4000) and flash-cryocooling. Unfortunately, the freezing protocol proved hard to reproduce, possibly because crystal dehydration in cryobuffer depended too sensitively on soaking time.

The best in-house specimen was tested on BW6, DESY, but no further improvement of resolution was seen and therefore no synchrotron dataset was collected. With the $P3_221$ model of PNP-II, this orthorhombic crystal form was easily solved by molecular replacement with AMoRe, assuming space group $P2_12_12$, and choosing the two longer axes as screw axes consistent with extinctions on the 00-lines in reciprocal space. With the correct space group, the initial *R*-factor after molecular replacement was 38% and the intensity correlation 63%, whereas for any other choice of screw axes the top "solution" had at least a 10% higher *R*-factor and a correlation no larger than 45%. Crystals could also be grown in the presence of Xan, but we could not repeat the dehydration protocol to improve their diffraction limit. In contrast to the trigonal crystal form, there is robust electron density for the phosphate and guanine ligands that were present in the crystallization buffer. The final model for this crystal form comprises residues 5–277 in all protomers, and the phosphate and guanine ligands in all subunits.

Crystals could also be grown with Hampton research cryobuffer 17 (150 mM Li_2SO_4, 85 mM Tris (pH 8.5), 25.5% PEG 4000, 15% glycerol), and were orthorhombic with cell dimensions 93.4 Å, 150.4 Å, 155.2 Å and two trimers in the asymmetric unit. Having observed an identical mode of dimerization of two trimers in the other two conditions, we took the hexameric species as the search model and found a very clear molecular replacement solution in space group $P2_12_12$ with both long axes taken as screws consistent with extinctions. The diffraction limit for these crystals was about 3.2 Å, but gratifyingly useful crystals could be grown in the presence of Xan. The deposited model contains residues 5–60 and 68–277 for all six subunits in the asymmetric unit, together with models for the xanthine and sulfate ligands from the crystallization buffer.

Because of the relatively poor diffraction of all three crystal forms, all models were refined with NCS-restraints. The final models have acceptable *R*-factors and stereochemistry (Table 1).

Protein Data Bank accession codes

Structure factors and coordinates for the three crystal forms have been submitted to the RCSB Protein Data Bank under accession codes 1YQU (trigonal form with guanine and phosphate), 1YQQ (small orthorhombic form with guanine and phosphate) and 1YR3 (large orthorhombic form with xanthine and sulfate).

Acknowledgements

We thank Victor Lamzin and Paul Tucker of the Hamburg EMBL outstation at DESY for generous allocation of beam time, and Peter Zwart and Max Lowe for assistance with data collection, Vern Schramm for providing the hPNP expression plasmid, and Nina Jensen for excellent technical assistance. Generous access to BW6 at DESY, Hamburg and help from Hans Bartunik and Gleb Bourenkov are also gratefully acknowledged. This work was supported, in part, by the Ministry of Scientific Research and Information Technology (MNiI), grants 3PO4AO2425 and KO89/PO4/2004.

References

1. Bzowska, A., Kulikowska, E. & Shugar, D. (2000). Purine nucleoside phosphorylases: properties, functions, and clinical aspects. *Pharmacol. Ther.* **88**, 349–425.
2. Buxton, R. S., Hammer-Jespersen, K. & Valentin-Hansen, P. (1980). A second purine nucleoside phosphorylase in *Escherichia coli* K-12. I. Xanthosine phosphorylase regulatory mutants isolated as secondary-site revertants of a deoD mutant. *Mol. Gen. Genet.* **179**, 331–340.
3. Hammer-Jespersen, K., Buxton, R. S. & Hansen, T. D. (1980). A second purine nucleoside phosphorylase in *Escherichia coli* K-12. II. Properties of xanthosine phosphorylase and its induction by xanthosine. *Mol. Gen. Genet.* **179**, 341–348.
4. Bezirjian, K. O., Kocharian, S. M. & Akopyan, Z. I. (1986). Isolation of a hexameric form of purine nucleoside phosphorylase II from *E. coli*. Comparative study of trimeric and hexameric forms of the enzyme. *Biokhimia*, **51**, 1085–1092.
5. Hershfield, M. S., Chaffee, S., Koro-Johnson, L., Mary, A., Smith, A. A. & Short, S. A. (1991). Use of site-directed mutagenesis to enhance the epitope-shielding effect of covalent modification of proteins with polyethylene glycol. *Proc. Natl Acad. Sci. USA*, **88**, 7185–7189.
6. Pugmire, M. J. & Ealick, S. E. (2002). Structural analyses reveal two distinct families of nucleoside phosphorylases. *Biochem. J.* **361**, 1–25.
7. Koellner, G., Luic, M., Shugar, D., Saenger, W. & Bzowska, A. (1998). Crystal structure of the ternary complex of *E. coli* purine nucleoside phosphorylase with formycin B, a structural analogue of the substrate inosine, and phosphate (sulphate) at 2.1 Å resolution. *J. Mol. Biol.* **280**, 153–166.
8. Koszalka, G. W., Vanhooke, J., Short, S. A. & Hall, W. W. (1988). Purification and properties of inosine-guanosine phosphorylase from *Escherichia coli* K-12. *J. Bacteriol.* **170**, 3493–3498.
9. Stoychev, G., Kierdaszuk, B. & Shugar, D. (2002). Xanthosine and xanthine. Substrate properties with purine nucleoside phosphorylases, and relevance to other enzyme systems. *Eur. J. Biochem.* **269**, 4048–4057.
10. Poznanski, J., Kierdaszuk, B. & Shugar, D. (2003). Structural properties of the neutral and monoanionic forms of xanthosine, highly relevant to their substrate properties with various enzyme systems. *Nucleosides Nucleotides. Nucl. Acids*, **22**, 249–263.
11. Kulikowska, E., Kierdaszuk, B. & Shugar, D. (2004). Xanthine, xanthosine and its nucleotides: solution structures of neutral and ionic forms, and relevance to substrate properties in various enzyme systems and metabolic pathways. *Acta Biochim. Pol.* **51**, 493–531.
12. Cavalieri, L., Fox, J., Stone, A. & Chang, N. (1954). On the nature of xanthine and substituted xanthines in solution. *J. Am. Chem. Soc.* **76**, 1119–1122.
13. Roy, K. B. & Miles, H. T. (1983). Tautomerism and ionization of xanthosine. *Nucleosides Nucleotides*, **2**, 231–242.
14. Seeger, C., Poulsen, C. & Dandanell, G. (1995). Identification and characterization of genes (xapA, xapB, and xapR) involved in xanthosine catabolism in *Escherichia coli*. *J. Bacteriol.* **177**, 5506–5516.
15. Mao, C., Cook, W. J., Zhou, M., Federov, A. A., Almo, S. C. & Ealick, S. E. (1998). Calf spleen purine nucleoside phosphorylase complexed with substrates and substrate analogues. *Biochemistry*, **37**, 7135–7146.

16. Jones, S. & Thornton, J. M. (1996). Principles of protein–protein interactions. *Proc. Natl Acad. Sci. USA*, **93**, 13–20.
17. Singh, J. & Thornton, J. M. (1992). *Atlas of Protein Side-chain Interactions, I,II*, IRL Press, Oxford, UK.
18. Erion, M. D., Stoeckler, J. D., Guida, W. C., Walter, R. L. & Ealick, S. E. (1997). Purine nucleoside phosphorylase. 2. Catalytic mechanism. *Biochemistry*, **36**, 11735–11748.
19. Burley, S. K. & Petsko, G. A. (1985). Aromatic–aromatic interaction: a mechanism of protein structure stabilization. *Science*, **229**, 23–28.
20. Erion, M. D., Takabayashi, K., Smith, H. B., Kessi, J., Wagner, S., Honger, S. *et al*. (1997). Purine nucleoside phosphorylase. 1. Structure–function studies. *Biochemistry*, **36**, 11725–11734.
21. Colloc'h, N., el Hajji, M., Bachet, B., L'Hermite, G., Schiltz, M., Prange, T. *et al*. (1997). Crystal structure of the protein drug urate oxidase-inhibitor complex at 2.05 Å resolution. *Nature Struct. Biol.* **4**, 947–952.
22. Retailleau, P., Colloc'h, N., Vivares, D., Bonnete, F., Castro, B., El-Hajji, M. *et al*. (2004). Complexed and ligand-free high-resolution structures of urate oxidase (Uox) from *Aspergillus flavus*: a reassignment of the active-site binding mode. *Acta Crystallog. sect. D*, **60**, 453–462.
23. Maynes, J. T., Yam, W., Jenuth, J. P., Gang Yuan, R., Litster, S. A., Phipps, B. M. & Snyder, F. F. (1999). Design of an adenosine phosphorylase by active-site modification of murine purine nucleoside phosphorylase. Enzyme kinetics and molecular dynamics simulation of Asn-243 and Lys-244 substitutions of purine nucleoside phosphorylase. *Biochem. J.* **344**, 585–592.
24. Stoeckler, J. D., Poirot, A. F., Smith, R. M., Parks, R. E., Jr, Ealick, S. E., Takabayashi, K. & Erion, M. D. (1997). Purine nucleoside phosphorylase. 3. Reversal of purine base specificity by site-directed mutagenesis. *Biochemistry*, **36**, 11749–11756.
25. Singh, J. & Thornton, J. M. (1992). *Atlas of Protein Side-chain Interactions*, IRL Press, Oxford, UK.
26. Giacomello, A. & Salerno, C. (1978). Human hypoxanthine-guanine phosphoribosyltransferase. Steady state kinetics of the forward and reverse reactions. *J. Biol. Chem.* **253**, 6038–6044.
27. Yuan, L., Craig, S. P., McKerrow, J. H. & Wang, C. C. (1992). Steady-state kinetics of the schistosomal hypoxanthine-guanine phosphoribosyltransferase. *Biochemistry*, **31**, 806–810.
28. Donald, R. G., Carter, D., Ullman, B. & Roos, D. S. (1996). Insertional tagging, cloning, and expression of the *Toxoplasma gondii* hypoxanthine-xanthine-guanine phosphoribosyltransferase gene. Use as a selectable marker for stable transformation. *J. Biol. Chem.* **271**, 14010–14019.
29. Schumacher, M. A., Carter, D., Ross, D. S., Ullman, B. & Brennan, R. G. (1996). Crystal structures of *Toxoplasma gondii* HGXPRTase reveal the catalytic role of a long flexible loop. *Nature Struct. Biol.* **3**, 881–887.
30. Raman, J., Sumathy, K., Anand, R. P. & Balaram, H. (2004). A non-active site mutation in human hypoxanthine guanine phosphoribosyltransferase expands substrate specificity. *Arch. Biochem. Biophys.* **427**, 116–122.
31. Jorgensen, C. & Dandanell, G. (1999). Isolation and characterization of mutations in the *Escherichia coli* regulatory protein XapR. *J. Bacteriol.* **181**, 4397–4403.
32. Jones, T. A., Zou, J. Y., Cowan, S. W. & Kjeldgaard, M. (1991). Improved methods for building protein models in electron density maps and the location of errors in these models. *Acta Crystallog. sect. A*, **47**, 110–119.
33. Brunger, A. T., Adams, P. D., Clore, G. M., DeLano, W. L., Gros, P., Grosse-Kunstleve, R. W. *et al*. (1998). Crystallography and NMR system: a new software suite for macromolecular structure determination. *Acta Crystallog. sect. D*, **54**, 905–921.
34. Pfleiderer, W. & Nübel, G. (1961). Zur struktur des Xanthins und seiner *N*-Methyl-xanthin-derivate. *Ann. Chem.* **647**, 155–160.
35. Ames, B. N. (1966). Assay of inorganic phosphate. *Methods Enzymol.* **8**, 115–116.
36. Hansen, M. R. & Dandanell, G. (2005). Purification and characterization of RihC, a xanthosine-inosine-uridine-adenosine preferring hydrolase from *Salmonella enterica* serovar Typhimurium. *Biochim. Biophys. Acta*, in the press.

Edited by I. Wilson

(Received 13 October 2004; received in revised form 3 February 2005; accepted 4 February 2005)